STIRLING ENGINE OPERATING WITH SOLID WASTE IN RURAL AREA

Vo Anh Vu[1], Phung Minh Tung[2]*, Bui Van Ga[1], Nguyen Van Vu[1], Nguyen Van Dung[1], Nguyen Hieu[1], Doan Da Vu[1]

[1]*The University of Danang - University of Science and Technology, Vietnam*
[2]*The University of Danang - University of Technology and Education, Vietnam*

*Corresponding author: pmtung@ute.udn.vn

(Received: May 04, 2025; Revised: June 04, 2025; Accepted: June 21, 2025)

DOI: 10.31130/ud-jst.2025.23(9D).575E

Abstract - The use of syngas derived from biomass gasification as fuel for internal combustion engines presents significant challenges due to the presence of harmful impurities. However, syngas combustion offers an effective heat supply solution for external combustion engines, such as Stirling engines. This report details the design, fabrication, and testing of a gasifier-stirling engine system using rice husk-derived RDF as fuel. Rice husks are compressed into honeycomb-shaped pellets to improve biomass storage and enhance gasification efficiency. The Stirling engine can be heated directly by the combustion of RDF pellets or indirectly by syngas produced through the gasification of RDF in the gasifier. Initial results indicate that the difference between the simulated and experimental combustion temperatures of RDF is approximately 13%. The gasifier-Stirling engine system has been fully designed and manufactured, ready for testing in the next phase of experimentation.

Keywords - Syngas; Biomass; Stirling engine; RDF; Greenhouse gas

1. Introduction

Solid waste management remains a persistent challenge for most countries worldwide. Traditional landfilling continues to be the most prevalent waste treatment method; however, it presents significant disadvantages, including considerable land occupation [1], greenhouse gas emissions (primarily CO_2 [2] and CH_4 [3]), leachate generation, odour dispersion, and risks of fire, explosion, or landslides. These issues pose dangers to both the environment and human health [4]. Additionally, landfilling does not facilitate the recycling of valuable materials from waste [5].

Landfilling is now Vietnam's main method of managing trash, and the majority of landfills are overflowing. The processing of solid waste from daily activities and agricultural production is still insufficient in rural regions, which makes the situation especially dire and has a major negative influence on the environment. Therefore, finding a complete and sustainable waste treatment solution is crucial. The existing environmental protection legislation in Vietnam require that solid waste be separated at the source so that new technologies can be used in later stages of waste processing.

Traditional waste incineration methods are inefficient and require complex, costly exhaust gas treatment solutions. The conversion of combustible municipal solid waste fractions into Refuse Derived Fuel (RDF) and its utilization as an alternative fuel is emerging as a new trend in solid waste management [6]. The concept of RDF was developed in the early 1970s [7]. Converting waste to energy through RDF offers numerous practical benefits, such as promoting circular economy development, conserving land resources, enhancing resource utilization efficiency, and substituting fossil fuels with renewable energy [8]. Furthermore, the abundant and continuous waste source helps reduce dependence on imported fuel sources [9]. Moreover, approximately 50% of the carbon content in household and industrial waste is of renewable origin [10], thus utilizing energy from solid waste contributes to reducing greenhouse gas emissions [11].

RDF gasification presents an effective solution to overcome the disadvantages of direct incineration. During the gasification process, RDF is converted into synthesis gas (syngas), comprising CO_2, CO, H_2, CH_4, H_2O, and other hydrocarbon gases, soot, coke, and ash. After purification, syngas can be used to produce liquid hydrocarbon fuels, hydrogen, methanol, and ammonia, or serve as fuel for engines [12]. This process delivers higher energy recovery efficiency compared to direct combustion while reducing emissions [13].

Syngas from gasification contains impurities like tar, which harm internal combustion engines, making filtration essential. Alternatively, syngas can power external combustion engines, such as steam or Stirling engines. While steam engines are simple but inefficient, Stirling engines offer higher thermal efficiency—theoretically nearing Carnot efficiency. In practice, they achieve 30-40% efficiency, surpassing internal combustion engines (25-30%) due to no incomplete combustion losses, heat recovery via regenerators, and absence of valve friction or gas exchange processes.

Stirling engines can utilize heat from diverse sources, including renewables and waste heat, enhancing energy efficiency. They are widely used in solar thermal power (outperforming solar panels), industrial waste heat recovery (e.g., furnaces, cement plants), and small-scale biomass or stove-based generators, providing electricity to remote areas. In this research, we design a Stirling engine powered by thermal energy recovered from solid waste in agricultural and forestry production. The solid waste is processed into honeycomb-shaped RDF fuel pellets to increase fuel density, facilitate biomass storage, and improve combustion and gasification conditions of the biomass. The Stirling engine is directly heated by burning RDF pellets or by burning syngas obtained from the gasification process. The research content includes the production of honeycomb-shaped RDF pellets from biomass, designing and manufacturing a Stirling engine, and designing and constructing a gasifier for honeycomb-shaped fuel pellets.

2. Material and method

2.1. Simulation

The combustion process of fuel pellets was simulated using Ansys Fluent software version 21R1. The content focuses on basic research of the pellet combustion process, so the computational domain configuration consists of a cylindrical pellet with a diameter of 30mm and a height of 40mm placed within an air environment computational space to simulate the pellet combustion process in the heating furnace of a Stirling engine (Figure 1). Air is drawn in at the bottom surface of the cylinder due to gravitational force. The pellet is assumed to have a porous structure, compressed from rice husks with elemental composition by mass: C(50%), H(6%), O(43.6%), and N(0.4%). The fuel is introduced into the simulation according to its elemental composition. Based on this composition, we can calculate the air/fuel ratio r under theoretical complete combustion conditions.:

$$r = \frac{100}{23}\left(\frac{8x_C}{3} + 8x_H - x_O\right) \quad (1)$$

Which x_C, x_H, x_O represents the mass fractions of C, H, and O in fuel according to Table 1.

***Table 1.** Fuel Composition in RDF pellet.*

Fuel Pellet	Fuel composition (% by mass)			
	C	H	O	N
RDF-Husk	0.500	0.060	0.436	0.004
RDF-Solid waste	0.570	0.061	0.350	0.019
RDF-Wood chips	0.533	0.064	0.402	0.001

In this research, the *k-ω* turbulence model and the Partially Premixed Combustion model were selected. Within the computational domain, the air surrounding the pellet has a combustion progress parameter of $c = 1$, while inside the pellet $c = 0$. At the initiation of the simulation, these values are assigned using the Patch tool in the Initialization panel. The fuel composition f is assumed to be input as the initial value of the pellet. From this, the excess air ratio ER is determined:

$$ER = \frac{fr}{1-f} \quad (2)$$

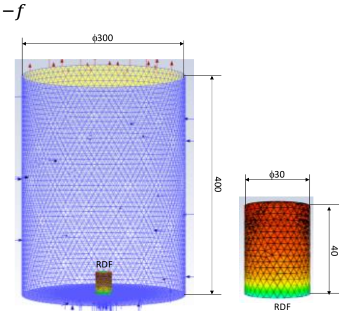

***Figure 1.** Meshing computational domain (a) and RDF pellet*

In this research, the combustion process parameters are determined, including the maximum values of temperature and concentrations of substances in the combustion products at each time point. Based on the mass composition of substances in the combustion products, we can calculate the calorific value of syngas according to the formula:

$$Q_{syn} = 10,16x_{CO} + 49,853x_{CH4} + 120,087x_{H2}\left(MJ/kg\right) \quad (3)$$

In which x_{CO}, x_{CH4}, x_{H2} represent the mass fractions (g/g) of CO, CH_4 and H_2.

2.2. Experimental

Const Stirling Engine Construction: Built with key components including hot/cold sections, a slider, and piston-cylinder assembly. Its heating furnace contains an RDF combustion chamber and a copper-tube heat exchanger.

Gasification Furnace Design: An updraft gasifier was developed to match the engine's power needs, with gasification zone sizing based on throat gas flow density.

Heat Measurement: RDF pellet combustion heat was measured and compared with simulation data.

3. Results and discussion

3.1. Combustion of RDF

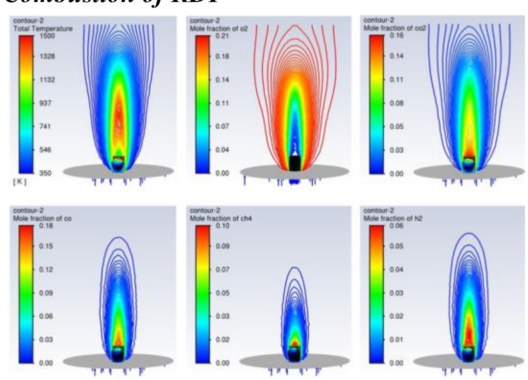

***Figure 2.** Contours of temperature, concentrations of CO, CH_4, and H_2 in the RDF-Rice husk Flame*

Figure 2 shows temperature contours and CO, CO_2, CH_4, and H_2 concentration profiles in the rice husk RDF flame. The highest temperatures and combustion product concentrations occur in the flame's front region. Under fuel-rich conditions, incomplete combustion results in partial conversion of carbon and hydrogen to CO_2 and H_2O, increasing CO, CH_4, and H_2 levels. These concentrations follow thermodynamic equilibrium principles. At stable combustion, peak molar concentrations reach 18% CO, 10% CH_4, and 6% H_2 (Figure 2).

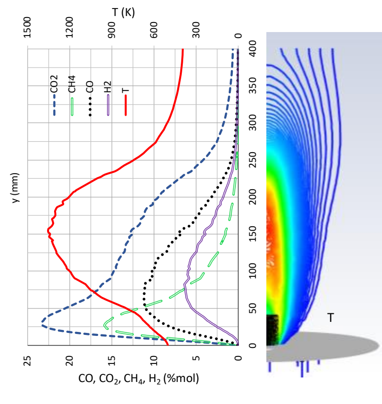

***Figure 3.** Distribution of H_2, CH_4, CO, CO_2 concentration and temperature T on the y-axis of RDF flame*

The variation of temperature and concentration of components along the axis of the rice husk RDF pellet is presented in Figure 3. It can be observed that the maximum concentrations of components are located closer to the RDF pellet than the maximum temperature. This can be explained by the fact that near the RDF pellet, the fuel-air mixture is fuel-rich, resulting in lower combustion temperatures but higher concentrations of incomplete combustion products. The gaseous fuel components CO, CH_4, and H_2 tend to reach maximum concentrations when 25 mm < y < 75 mm, corresponding to combustion temperature ranges from 700°C to 1050°C.

Figure 4a presents the temperature contour of the rice husk RDF flame. During combustion, oxygen from the air diffuses and reacts with the vaporized fuel from the RDF, causing the frontal region of the flame to be positioned outside the periphery of the RDF pellet. When y < 90 mm, the T(x) curve exhibits two peaks corresponding to the flame positions on the left and right sides of the pellet (Figure 4b). When y > 90 mm, the T(x) curve displays only one peak at the flame tip. The highest flame temperature occurs when y ranges from 90 mm to 150 mm. This region can be considered as the well-mixed zone between vaporized fuel from the RDF pellet and air. When y > 150 mm, the gas temperature decreases rapidly due to the diffusion of air into the combustion products.

The variation of CO, CH_4, and H_2 concentrations along the z-direction is similar to the flame temperature variation. Figure 5 presents graphs of component concentrations at y = 50 mm. The results indicate that the formation of CO, CH_4, and H_2 primarily occurs at the flame front. Subsequently, CO, CH_4, and H_2 rapidly diffuse into the surrounding air, thus their concentrations decrease to 0 at the outer edges of the flame..

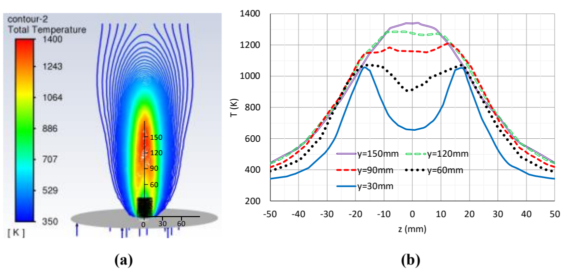

Figure 4. *Temperature distribution in flame of RDF. (a) Contour of temperature, (b) Variation of temperature in z direction*

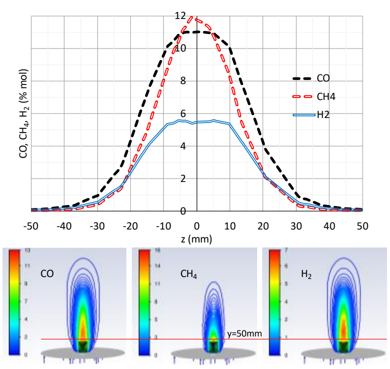

Figure 5. *Distribution of specie concentrations in z direction at y=50mm of RDF*

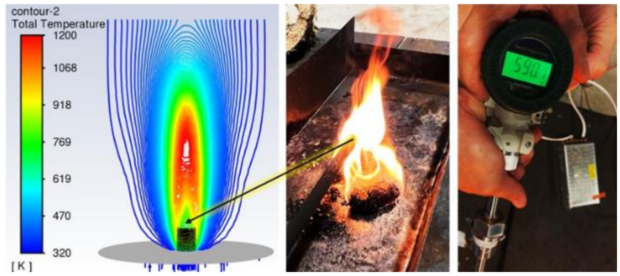

Figure 6. *Comparison of flame shape between simulation and experiment*

Figure 6 compares the flame shape of RDF-Rice Husk between simulation results and experimental observations. As the flame burns in an open-air environment, its frontal portion fluctuates (similar to an oil lamp flame). However, the basic shape of the flame burning from RDF resembles the pencil-like shape of a jet fuel gas flame. Thermal radiation from soot particles within the flame makes it visibly luminous. It can be observed that the flame shape in the simulation is similar to the experimental flame. This confirms the initial hypothesis regarding RDF combustion simulation: the combustion process of vaporized fuel emitted from the RDF pellet.

The average temperature of the RDF combustion process was measured using a thermocouple. This is a specialized instrument for temperature measurement in boilers or gasification furnaces. Figure 7 presents the average temperature inside the RDF-Rice Husk pellet. The experimental value is 738K, compared to the simulation value of 850K. The average temperature deviation between the two values is 13%.

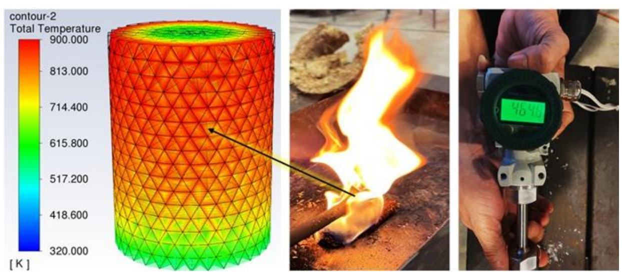

Figure 7. *Comparison of average temperature given by simulation and experiment of RDF-Rice husk flame.*

3.2. Combustion of syngas

The case of utilizing syngas as fuel for the Stirling engine involves syngas obtained from the gasification process using a downdraft fixed-bed gasifier with RDF pellets as the input feedstock.

Figure 8. *Figure depicting the syngas flame combustion at the gasifier outlet*

Figure 8 demonstrates the syngas flame at the gasifier outlet after the gasifier has reached stable operation. Figure

16 presents the composition of constituent gases in the syngas measured using a Gasboard-3100P gas analyzer. It can be observed that the syngas obtained from the downdraft gasifier exhibit high quality.

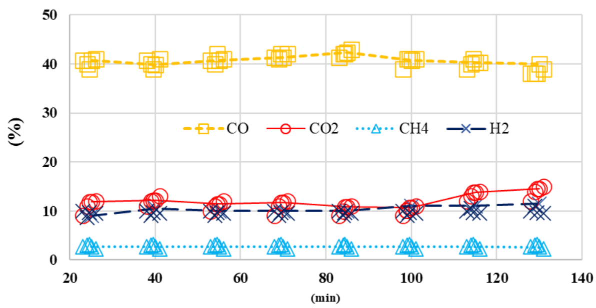

Figure 9. *The composition of syngas obtained from the gasification process of RDF pellets using a downdraft fixed-bed gasifier*

The results obtained from the gas composition analyzer, as shown in Figure 9, indicate that the combustible gas components constitute approximately 50% of the total composition. Experimental results demonstrate that syngas can effectively serve as a fuel for the Stirling engine.

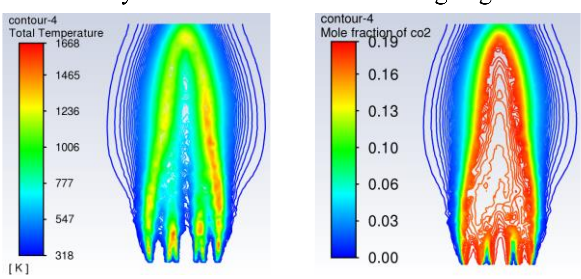

a) *b)*

Figure 10. *The flame temperature and the CO_2 concentration distribution*

When combusting syngas in the combustion chamber to supply heat to the Stirling engine, the flame temperature profile is depicted in Figure 10a, and the CO_2 concentration distribution is illustrated in Figure 10b. We observe that the maximum flame temperature reaches approximately 1668K, occurring in the region with optimal mixture composition. As compared to the flame of RDF combustion (1400K), the temperature of syngas combustion is significantly higher. This is interesting for energy supply to Stirling engine.

Figure 11b shows the variation in flame temperature in the y-direction, while Figure 11a shows the variation in flame temperature along the x-direction. The region of ideal mixture composition is where the greatest temperature is found in the saddle-shaped contour of the flame temperature profile along the x-direction. The flame temperature progressively rises with altitude, peaking at the flame apex—the area with the ideal combination composition.

An average flame temperature of about 1200K may be reached while heating the Stirling engine with syngas flame, as this simulation result shows.

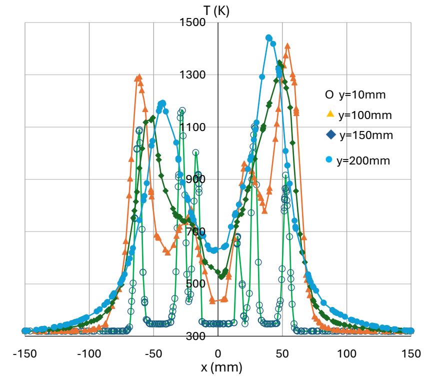

(a)

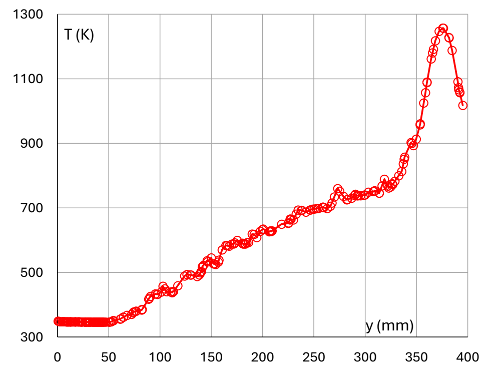

(b)

Figure 11. *a) The flame temperature variation along the x-direction, b) The flame temperature variation along the y-direction*

3.3. Stirling engine design

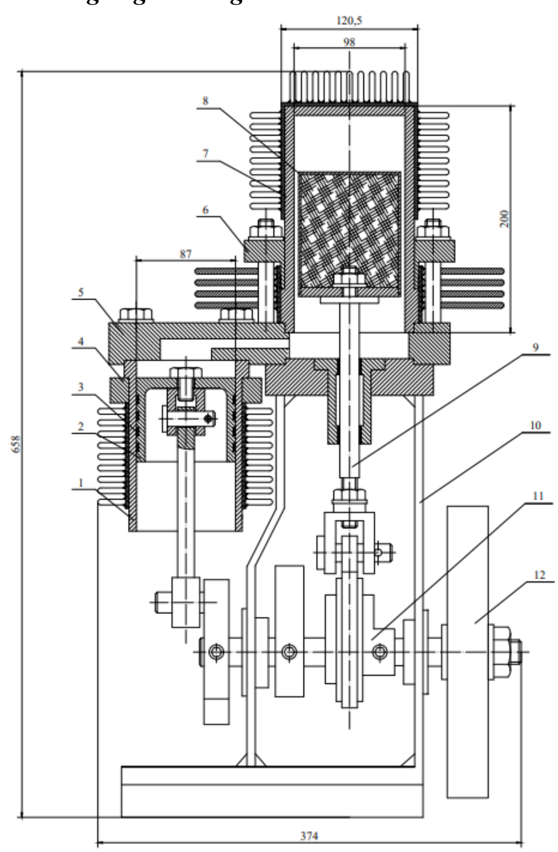

(a)

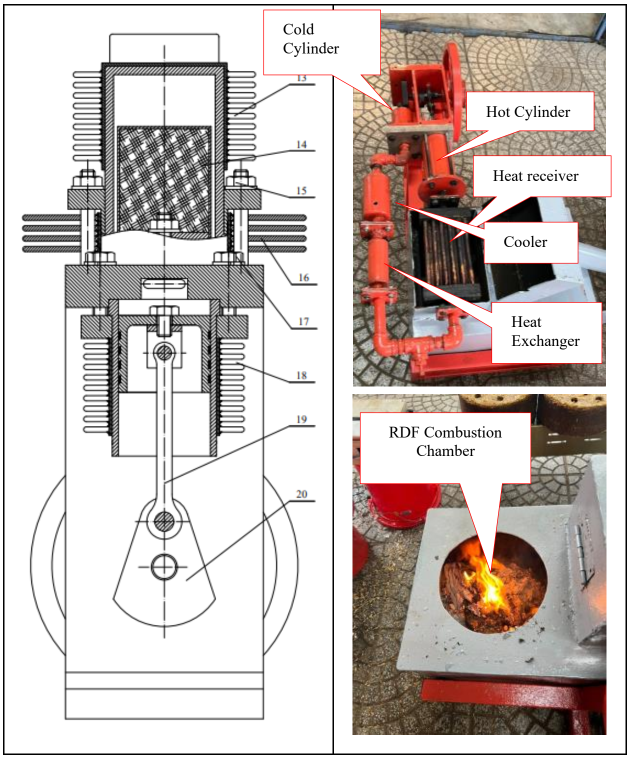

(b) (c)

Figure 12. *Technical drawing of the longitudinal cross-section (a) and transverse cross-section (b) of the Stirling engine, and the actual photograph of the Stirling engine used in the experiment(c)*

Figure 12 (a), (b), and (c) presents the assembly drawing and photograph of the Stirling engine after fabrication. The engine, with a cylinder volume of 1 liter, is designed to operate at a rotational speed of 3600 rev/min.

3.3.1. Calculating the Power of the Stirling Engine:

When a heat engine operates between two heat sources at TH=1300K (hot source) and TC=320K (cold source), its Carnot efficiency is:

$$\eta_{Carnot} = 1 - \frac{T_C}{T_H} = 1 - \frac{320}{1300} \approx 0.754 \quad (4)$$

The actual efficiency of the Stirling engine is less than the Carnot efficiency. If the efficiency coefficient of the engine is chosen as 0.4, then the thermal efficiency of the engine is:

$$\eta_{thuc} = 0.4 \times \eta_{Carnot} = 0.4 \times 0.754 \approx 0.302 \quad (5)$$

To calculate the cycle work, we need to determine the number of moles of working gas. Assuming the average pressure in the cycle is 1 atm (101325 Pa) and the average volume is 1 liter (0.001 m³). With an average temperature of T, the ideal gas state equation allows us to derive the number of moles of air acting as the working medium in the engine:

$$PV = nRT \Rightarrow n = \frac{PV}{RT} = \frac{101325 \times 0.001}{3.814 \times 810} \approx 0.015(mol) \quad (6)$$

Ideal cycle work W_{ideal}:

$$W_{ideal} = nR(T_H - T_C) = 0.015 \times 8.314 \times (1300 - 320) \times \ln(2) \approx 84.7(J) \quad (7)$$

Actual cycle work W_{thuc}:

$$W_{thuc} = \eta_{thuc} \times W_{ideal} = 0.302 \times 84.7 \approx 25.6(J) \quad (8)$$

Number of cycles executed per second:

$$N = \frac{3600(rev/min)}{60(sec/min)} = 60(rev/sec) \quad (9)$$

Engine power:

$$\boldsymbol{P = W_{thuc} \times N = 25.6(J/ct) \times 60}(ct/sec) = 1536W \approx 1.54kW \quad (10)$$

3.4. Experimental Compression of Honeycomb-Structured RDF Rice Husk pellets

Figure 13 (a) and (b) show the press machine, compression mold, and final honeycomb-structured RDF pellets made from compressed rice husks. The steel compression mold is electrically heated to 130-200°C and uses a 50-ton hydraulic cylinder for compression. The mold's movable face has welded 20mm iron posts that form the honeycomb pattern.

Loose rice husks are poured into the mold, compressing to 1/10th of their original volume. This significant size reduction makes the RDF pellets much easier to store and transport than uncompressed husks.

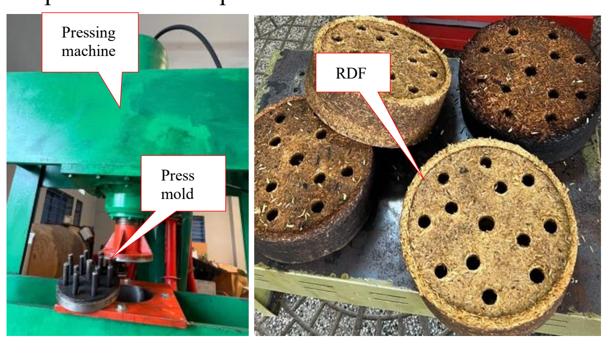

(a) (b)

Figure 13. *Pressing machine, honeycomb-shaped RDF rice husk pellet molding die (a) and honeycomb-shaped RDF rice husk pellet products after pressing (b).*

Figure 14. *RDF rice husk pellets during combustion (a) and after combustion (b)*

Figure 14 (a,b) illustrates that during the combustion process, flames appear at the honeycomb holes where air passes through. Consequently, the honeycomb RDF pellets facilitate uniform biomass combustion throughout the entire fuel volume. The honeycomb-shaped rice husk RDF burns very completely. After combustion, only ash remains, which can be used as fertilizer for plants.

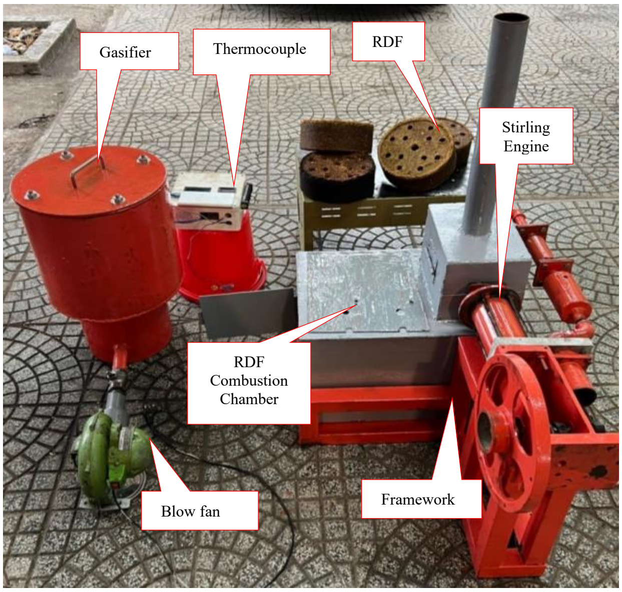

Figure 15. *Gasifier – Stirling Engine systems in experimental*

Figure 15 introduces the gasification furnace system and Stirling engine powered by honeycomb-structured rice husk RDF pellets after completion of fabrication.

4. Conclusions

To process rice husks into honeycomb-shaped RDF pellets, it is necessary to heat the mold to temperatures ranging from 130°C to 200°C with a compression force of 50 tons.

When compressed into RDF pellets, the volume of rice husks is reduced tenfold, facilitating easier biomass storage and transportation.

Rice husk RDF exhibits complete combustion characteristics and is readily gasifiable. The combustion temperature of rice husk RDF as determined by simulation differs from experimental results by approximately 13%.

The Stirling engine features a simplified structure that can be designed and manufactured using domestic technology. The engine can utilize RDF directly or indirectly through syngas obtained from the RDF gasification reactor.

The temperature of syngas flame is about 250K higher than that of RDF combustion, which effectively improves Stirling engine performance.

Acknowledgments: The authors wish to express their appreciation to the Ministry of Education and Training Vietnam for supporting this research under the project B2024.DNA.12, entitled "Smart controller for engine fueled with flexible gaseous fuels in hybrid renewable energy system”.

REFERENCES

[1] S. Chalermcharoenrat, K. Laohalidanond, and S. Kerdsuwan, "Optimization of Combustion Behavior and Producer Gas Quality from Reclaimed Landfill Through Highly Densify RDF-Gasification", *Energy Procedia*, vol. 79, pp. 321-326, 2015, doi: 10.1016/j.egypro.2015.11.496.

[2] H. Rezaei, F. Panah, J. Lim, and S. Sokhansanj, "Pelletization of Refuse-Derived Fuel with Varying Compositions of Plastic, Paper, Organic and Wood", *Sustainability*, vol. 12, pp. 4645, 2020, doi: 10.3390/su12114645

[3] M. Kara, "Environmental and economic advantages associated with the use of RDF in cement kilns", *Resources, Conservation and Recycling*, vol. 68, pp. 21-28, 2012, doi: 10.1016/j.resconrec.2012.06.011.

[4] M. R. Boni, A. Chiavola, and S. Sbaffoni, "Pretreated waste landfilling: Relation between leachate characteristics and mechanical behaviour", *Waste Management*, vol. 26, pp. 1156-1165, 2006, doi: 10.1016/j.wasman.2006.01.001.

[5] Z. Xu, A. Elomri, S. Pokharel, Q. Zhang, X. G. Ming, and W. Liu, "Global reverse supply chain design for solid waste recycling under uncertainties and carbon emission constraint", *Waste Management*, vol. 64, pp. 358-370, 2017, doi: 10.1016/j.wasman.2017.02.024.

[6] P. M. Tung, B. V. Ga, and T. T. Son, "Experimental study of RDF production from solid waste", *Proceedings of the 24th National Coference in Fluid Machanic*, *Hanoi-Danang-HoChiMinh City*, *18-12-2021*, Natural Science and Technology Publishing House, 2021, pp. 595-604.

[7] K. Daugherty, "An Identification of Potential Binding Agents for Densified Fuel Preparation from Municipal Solid Waste: Phase 1", Argonne National Lab.IL, USA, Final report, 1986.

[8] A. S. Akdağ, A. Atimtay, and F. D. Sanin, "Comparison of fuel value and combustion characteristics of two different RDF samples", *Waste management*, vol. 47, pp. 2015, doi: 10.1016/j.wasman.2015.08.037.

[9] D. T. Pio, L. A. C. Tarelho, A. M. A. Tavares, M. A. A. Matos, and V. Silva, "Co-gasification of refused derived fuel and biomass in a pilot-scale bubbling fluidized bed reactor", *Energy Conversion and Management*, vol. 206, pp. 112476, 2020, doi: 10.1016/j.enconman.2020.112476.

[10] L. Lombardi, E. Carnevale, and A. Corti, "A review of technologies and performances of thermal treatment systems for energy recovery from waste", *Waste Management*., vol. 37, pp. 26-44, 2014.

[11] R. Luque and J.G. Speight, "Gasification for Synthetic Fuel Production", 2015.

[12] A. K. Dalai, N. Batta, I. Eswaramoorthi, and G. J. Schoenau, "Gasification of refuse derived fuel in a fixed bed reactor for syngas production", *Waste Management*, vol. 29, pp. 252-258, 2009, doi: 10.1016/j.wasman.2008.02.009.

[13] S. Galvagno *et al.*, "Steam gasification of tyre waste, poplar, and refuse-derived fuel: A comparative analysis", *Waste Management*, vol. 29, pp. 678-689, 2009, doi: 10.1016/j.wasman.2008.06.003.